

Atlas motion platform split-axle mecanum wheel design¹

Jane M. Schwering, Mila J.E. Kanevsky, M. John D. Hayes, and Robert G. Langlois

Abstract: The Atlas motion platform was conceptually introduced in 2005 as a 2.90 m diameter thin-walled composite sphere housing a cockpit. Three active mecanum wheels provide three linearly independent torque inputs enabling the sphere to enjoy a 100% dexterous reachable workspace with unbounded rotations about any axis. Three linearly independent translations of the sphere centre, decoupled from the orientation workspace, are provided by a translational three degree-of-freedom platform. Small-scale and half-scale demonstrators introduced in 2005 and 2009, respectively, gave us the confidence needed to begin the full-scale design. Actuation and control of the Atlas full-scale design is nearing completion; however, resolution of several details have proven extremely elusive. The focus of this paper is on the design path of the 24 passive mecanum wheels. The 12 passive wheels below the equator of the sphere help distribute the static and dynamic loads, while 12 passive wheels above the equator, attached to a pneumatically actuated halo, provide sufficient downward force so that the normal force between the three active wheel contact patches and sphere surface enable effective torque transfer. This paper details the issues associated with the original twin-hub passive wheels and the resolution of those issues with the current split-axle design. Results of static and dynamic load tests are discussed.

Key words: Atlas motion platform, mecanum wheel, twin-hub and split-axle.

Résumé : La plate-forme mobile Atlas fut introduite conceptuellement en 2005 comme une sphère composite à paroi mince d'un diamètre de 2,90 m à l'intérieur de laquelle était installé un poste de pilotage. Trois roues de type mecanum génèrent trois couples d'entraînement linéairement indépendants fournissant à la sphère une dextérité totale sur l'ensemble de son espace atteignable ainsi que des rotations non bornées par rapport à tous les axes. Trois mouvements de translation indépendants du centre de la sphère, qui sont découplés par rapport à sa rotation, sont fournis par une plate-forme linéaire à trois degrés de liberté. Les résultats obtenus à partir de prototypes démonstrateurs à petite et moyenne échelle, développés respectivement en 2005 et en 2009, justifient le développement d'un prototype à pleine échelle. Quoique les tâches d'actionnement et de commande du prototype à pleine échelle du système Atlas s'achèvent, certaines difficultés furent encourues avec la résolution de quelques détails. Cet article porte sur la conception des 24 roues passives de type mecanum. Les 12 roues situées en dessous du cercle équatorial de la sphère contribuent à distribuer les charges statiques et dynamiques. Pour leur part, les 12 roues situées au-dessus du cercle équatorial de la sphère, qui sont attachées à un anneau à actionnement pneumatique, transmettent une force suffisante vers le bas pour engendrer les forces normales nécessaires entre les surfaces de contact des roues actives et la surface de la sphère pour permettre la transmission de couples. Les résultats d'essais expérimentaux avec chargement sont discutés. [Traduit par la Rédaction]

Mots-clés : la plate-forme mobile Atlas, roues de type mecanum, roues à demi-essieu.

1. Introduction

This paper represents the unstable ground between the two age-old mechanical engineering design adages:

paper design is patient and; the devil is in the details. The Atlas motion platform was conceptually introduced in 2005 (Hayes and Langlois 2005; Holland et al. 2005;

Received 12 July 2019. Accepted 10 September 2019.

J.M. Schwering, M.J.E. Kanevsky, M.J.D. Hayes,* and R.G. Langlois. Department of Mechanical and Aerospace Engineering, Carleton University, Ottawa, ON K1S 5B6, Canada.

Corresponding author: M. John D. Hayes (email: john.hayes@carleton.ca).

¹This paper is part of a Special Issue with the best papers presented during the 2019 CCToMM Symposium on Mechanisms, Machines, and Mechatronics.

*M. John D. Hayes currently serves as a Guest Editor; peer review and editorial decisions regarding this manuscript were handled by Scott Nokleby.

Copyright remains with the author(s) or their institution(s). Permission for reuse (free in most cases) can be obtained from copyright.com.

Robinson et al. 2005). Atlas is largely a product of the Carleton University Simulator Project (CUSP) that started as one of six, now 11, full academic year-long 4th year capstone design projects in the Department of Mechanical and Aerospace Engineering at Carleton University in September 2002. These capstone design projects are ambitious, interdisciplinary, multi-year design projects managed by a small design office. A Project Manager, two or three additional faculty members, and a graduate student Teaching Assistant act as Lead Engineers supervising 15–25 4th year Mechanical and Aerospace Engineering students. The original long-term objectives of CUSP were to develop a complete and flexible simulation facility located at Carleton University, including a variety of mathematical models, a multi-functional motion platform, a general vision system, and a reconfigurable user interface all interoperating based on the IEEE standard for high-level architecture (IEEE Standard 2000; Chao et al. 2004).

The motion platform design objective in 2002 was to develop a novel concept for an architecturally-novel six degree-of-freedom (DOF) motion platform with a completely decoupled orientation and translation workspace, which was intended to address the orientation workspace limits imposed by the standard Gough–Stewart hexapod used almost exclusively for flight simulation motion platforms. By January 2003, the Atlas motion platform concept was conceived. Over the years, faculty members and students from departments such as Cognitive Science, Industrial Design, Computer and Systems Engineering, and Electrical Engineering have made contributions to advancing the evolution of the Atlas concept from a 20.32 cm (8 in.) diameter table top demonstrator, to a 1.22 m (4 ft) diameter technology demonstrator, all the way to the full-scale 2.90 m (9.5 ft) diameter prototype, a rendered solid model of which is illustrated in Fig. 1.

Based on the performance of the smaller-scale proof-of-concept demonstrators, the CUSP group commenced the detail design of the Atlas full-scale prototype in 2011 and manufacturing began in earnest in 2013. The detail design, manufacture, and assembly of all of the individual components are slowly approaching completion; the pace being an artifact of the timing imposed by the 4th year capstone design project paradigm. In this paper, the redesign, manufacture, and testing of the 12.70 cm (5 in.) diameter passive mecamum wheels are detailed.

The Atlas full-scale prototype is a six DOF motion platform with a completely decoupled orientation and translation workspace. A 2.90 m (9.5 ft) diameter thin-walled S-glass composite sphere houses a pilot seated in a cockpit. S-glass, S for strength, was selected as it is commonly used to provide greater strength with less weight than E-glass (Wallenberger and Bingham 2010). The orientation workspace is generated by three active mecamum wheels, originally omni-wheels, which provide three linearly independent torque inputs.

Fig. 1. Atlas motion platform. [Colour online.]

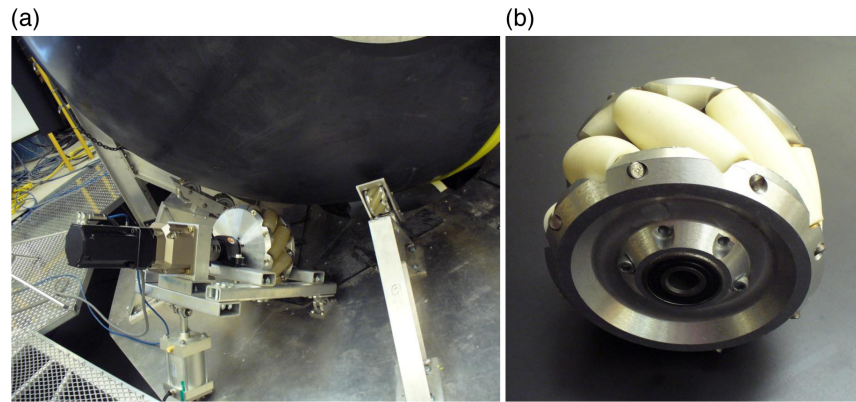


The sphere rotation actuation system and constraint mechanical system are all rigidly attached to an interface platform that, in turn, is rigidly attached to a MOOG MB-EP-6DOF Gough–Stewart platform (Gough 1956; Stewart 1965). The MOOG control system enables us to use only the 3D translation workspace to provide linear displacement of the sphere centre, hence the decoupled orientation and translation workspaces.

There are several other six DOF motion platforms that claim to have unbounded orientation workspaces such as the Desdemona (Bles et al. 2000) and Eclipse II (Kim et al. 2002) platforms. However, the Desdemona platform architecture relies on gimbals to generate the orientation workspace, which necessarily contains singular configurations related to gimbal lock, while the Eclipse II kinematic architecture imposes constraints on its orientation workspace caused by structural interferences, and rotation limits of the spherical joints. In contrast, the Atlas sphere interacts with the mecamum wheels through simple contact such that there are no joints or levers constraining its motion. This allows full 360° rotation about any axis in the workspace reachable by the sphere centre. As the MOOG platform can translate the sphere centre to all locations in its translation workspace and can attain any orientation about any axis in its rotation then, by definition (Pond and Carretero 2007), the reachable workspace is 100% dexterous.

As illustrated in Fig. 1, the Atlas orientation actuation system consists of the following: three 45.72 cm (18 in.) diameter active mecamum wheels mounted to the interface platform below the equator 120° apart, which are used to change the orientation of the sphere about its geometric centre; 12 lower 12.70 cm (5 in.) diameter passive mecamum wheels mounted to the interface platform

Fig. 2. Carleton University Simulator Project (CUSP) mecanum wheels. (a) Active and lower passive wheels. (b) Original twin-hub design. [Colour online.]



in pairs on rocker panels; 12 upper 12.70 cm (5 in.) diameter passive mecanum wheels hung in a circle parallel to the sphere equatorial plane at intervals of 30° from the circular halo suspended from the upper triangle attached to the three vertical uprights; two separate pneumatic systems that (i) push the upper mecanum wheels downward to press the sphere against the lower passive and active wheels, and (ii) push the lower active wheels upwards against the sphere to ensure that there is a 6675 N (1500 lb_f) normal force between the sphere and the three active wheels.

Originally, the passive and active mecanum wheels were designed as scaled versions of each other, see Fig. 2a. Each wheel consists of two identical outer hubs and a smaller diameter central hub to which the outer hubs are attached with shoulder bolts, see the passive wheel illustrated in Fig. 2b. Near the circumference of each outer hub are drilled eight through-castor-roller axle bearing holes at a 45° angle with respect to the wheel axle. These eight holes are repeated at 45° intervals on the same bolt circle. The passive polyurethane castor rollers were injection moulded around their axles with enough axle length on either side of the roller ends to allow them to be sandwiched together between the two outer hubs. Several unanticipated design issues arose at the passive roller axle bearings on the twin-hubs, along with the castor roller geometry, when the full-scale prototype was initially operated. The identified issues were significant enough to warrant a complete redesign of the passive wheels. Detailing these issues and their resolution with the redesigned passive mecanum wheels comprise the bulk of this paper. Additionally, empirical results from aggressive static and dynamic load case testing to destruction of the first prototype of the new split-axle passive wheel design will be presented and discussed.

2. Mecanum wheel design history

The mecanum wheel is commonly associated with ground vehicles that can turn with zero turning radius.

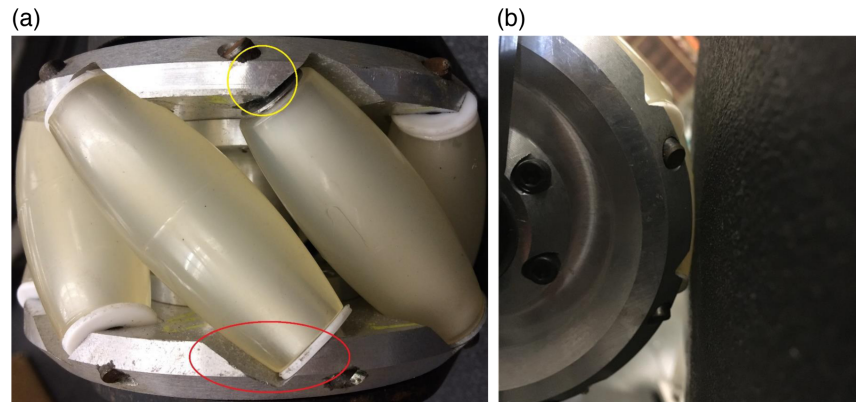
They are also known as Ilon wheels, after the Swedish inventor Bengt Ilon, who imagined the idea in 1973 when he was an engineer with the Swedish company Mecanum AB (Ilon 1975). They are conventional wheels with a series of castor rollers mounted to the periphery of the wheel's circumference. When the castor roller axles are rotated 45° relative to the wheel rotation axis they are called mecanum wheels, otherwise when the castor roller axles are at 90° relative to the wheel rotation axis they are known as omnidirectional wheels. Either version is designed to provide grip in the axial direction of the free-spinning castor rollers while allowing passive motion in all other directions, which causes the castor roller to spin about its axis. Until the introduction of the Atlas concept, mecanum and omnidirectional wheels were only ever used to move planar ground vehicles relative to the plane of the relatively stationary ground (Hayes and Langlois 2005). Because a plane can be considered a sphere with an infinite radius, it was reasoned that these wheels could be used to change the orientation of a sphere if the mecanum wheels were instead held in place and used as actuators to move the surface they contact (Hayes and Langlois 2005; Holland et al. 2005; Robinson et al. 2005). Indeed, the geometry of the mecanum wheels (Gfrerrer 2008) confirms that three linear combinations of active wheel angular velocity vectors with relatively constant direction cosines will spin the sphere about a central axis established by the linear combination of wheel speeds (Plumpton et al. 2014).

In what follows, we will discuss the significant operational issues identified with the original passive wheel structural design compounded by the selection of castor roller polyurethane durometer and roller geometry once the full-scale prototype sphere was in place; options considered; and finally, the significant design revision.

2.1. Twin-hub passive mecanum wheel design and associated issues

Originally, the passive mecanum wheel had two side plates that functioned as outer hubs securing the eight

Fig. 3. Twin-hub passive mecanum wheel issues. (a) Thin wall locations circled. (b) Hub almost touching sphere with no load. [Colour online.]



polyurethane rollers at 45° relative to the wheel rotation axis, see Fig. 2b. To accommodate the roller geometry, bearing holes and notches were machined on the inside faces of the hubs. The roller axles were lightly press fit in the bearing holes. The loose fit between the polyurethane castor roller and axle allowed the roller to spin on its axle. However, the notches made the hub wall thickness between the axle bearing hole and outside circumference perilously thin. The thin wall locations are circled in Fig. 3a.

The original design was also very difficult and time consuming to manufacture and even more difficult to assemble. The machining difficulty stems from the compound 45° angles of the notches and axle bearing holes along with the flats required by the six shoulder bolts used to fasten the two outer and one inner hub together. The assembly difficulties arise from the alignment of the 16 passive roller axle bearing holes in the two outer hubs, while simultaneously aligning the six shoulder bolt holes in all three hubs. Indeed, because of tolerance stackups most of the 24 passive mecanum wheels were held together by four shoulder bolts, while the one shown in Fig. 2b could only accommodate two. This problem, in turn, made it very difficult to disassemble to replace rollers.

However, another problem with the original passive wheel design was identified that was of far greater concern when the passive wheels were in use either supporting the static and dynamic loads or applying downward force to create the desired normal force between the active wheel rollers and sphere. When the passive mecanum wheels were supporting the sphere, the rollers deflected, as intended, but the combined effect of the 77A durometer polyurethane and radius of curvature of the passive rollers led to deflections that enabled the solid 6061 T6 aluminum outer wheel hubs to contact the sphere, thereby potentially damaging the composite shell. Of even greater concern was the issue illustrated in Fig. 3b. Even when the passive mecanum wheel was simply rested against the sphere without any load there was

little clearance between the wheel hubs and sphere. This was underscored when a piece of paper was placed between the two. When the paper was carefully removed it got caught on the hubs ultimately ripping the paper. This led to the conclusion that the sphere surface would be damaged by the passive wheel hubs, potentially significantly and irreparably if the platform were to be moved with its operational loads.

2.2. Mecanum wheel redesign

As the original twin-hub passive wheels were not suited for their intended use with the sphere, a new mecanum wheel design was needed. The initial thought was to redesign the original twin-hub passive wheel by increasing the castor roller curvature and increasing the diameter of the outer hubs to increase the wall thickness at the notches and axle mount locations. This would decrease the large stress concentrations in the hubs and help distribute it. However, this represented a contradiction because the increased roller curvature, while maintaining the 12.70 cm (5 in.) diameter of the wheels so they would fit the existing mounts, meant that material needed to be removed from the hub diameter to prevent the hubs from contacting the sphere. We also temporarily considered increasing the polyurethane durometer to make the castor rollers stiffer, which would result in decreased roller deflection under loading thereby decreasing the likelihood of the hubs contacting the sphere. It turned out, however, that the durometer of the polyurethane rollers could not be increased because the injection mould system injectors could not cope with the increased material resistance at the mould injection sites. The inescapable conclusion was that the existing twin-hub passive wheels could not be adequately modified, so the best option was to scrap them and start over.

One possible alternative to an outright new design was to consider commercially available wheels. Reasonably comprehensive research of commercial options yielded variants of split-axle mecanum wheels,

Fig. 4. VEX Robotics split-axle mecanum wheel.



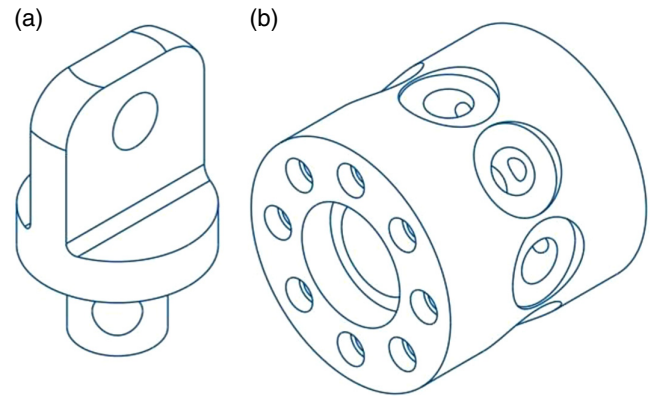
such as those offered by VEX Robotics, see Fig. 4. The split-axle wheels offered by VEX Robotics are only available in two sizes: 10.16 cm (4 in.) and 15.24 cm (6 in.). It turned out, however, that these were the best suited wheels that could be identified on the market. Unfortunately, the plastic components these wheels are formed with limit the load capacity rating for each 15.24 cm (6 in.) wheel to 222 N (50 lb_f). Since this is greater than an order of magnitude less the required load capacity, commercial options seemed to indicate outright redesign was inevitable. It was decided to test one of the purchased 15.24 cm (6 in.) wheels under static loading. The wheel failed under a static load of slightly greater than 800 N (180 lb_f). Regardless, the split-axle configuration presented a design option for the passive wheels that was worth examining in greater detail. The decision was made to investigate the split-axle design track. This decision immediately eliminated the potential contact between the hubs of the passive wheels and the sphere but at the expense of the uncertainty surrounding the cantilevered passive roller axle, and potential centre axle mount contact.

2.3. New design requirements

The decision to design a new split-axle 12.70 cm (5 in.) diameter passive wheel presented the opportunity to use the lessons learned from the unsuitability of the original twin-hub design to impose new requirements on the split-axle passive wheels to prevent similar problems from occurring. These new requirements included the following:

1. Design components for machined feature location and dimensional repeatability of $X.XXX \pm 0.001$ in. and $X.XXX \pm 0.005$ in. for all linear dimensions and

Fig. 5. New split-axle hub and castor roller mount. (a) New roller mount. (b) New hub. [Colour online.]



0.5° for all angular dimensions for all manufactured components (Imperial units were specified for tolerances because all purchased stock material dimensions, as well as machine tool systems were exclusively in Imperial units);

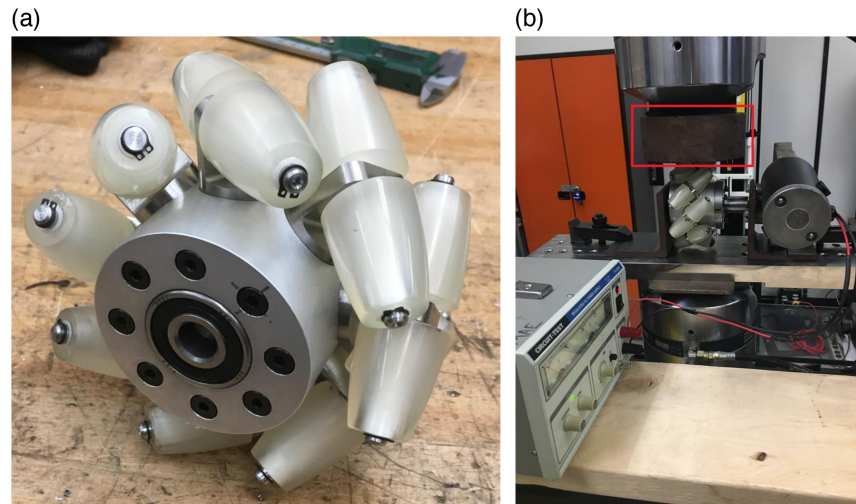
2. Withstand the maximum static and dynamic loads being caused by the sphere and its motion. Dynamic simulations estimate this maximum load to be 6675 N (1500 lb_f);
3. Must be dimensionally compatible with the current upper passive wheel hangers and lower mounts.

Once the new requirements were judged to be suitable and compatible with existing components, six different design options were iteratively examined and evaluated relative to the requirements. Exhaustive trade-off studies were conducted, and the conclusions led us to take the last revision to the detail design phase, leading to the fabrication of the first prototype split-axle passive wheel described next.

2.4. New split-axle design

The three features taken from the VEX Robotics wheel were the overall design simplicity, single hub, and the castor roller axle mounts centred on the hub circumference width. However, the design iterations led to a circular hub composed of 7050 aluminum instead of the octagonal hubs used by VEX Robotics. The main reason for a single circular hub was to reduce the reliance on tight tolerances needed for assembly of the twin-hub wheels. The new single piece hub was given the same width as the original three-piece hubs. The question was now how to attach the castor roller mounts to the hub. The answer, that the iterations converged to was to form the passive roller mounts as illustrated in Fig. 5a. The flange seats the mount on the hub in one of the mount countersinks drilled into the hub indexed at 45°. Each of eight mounts per hub is oriented at 45° by virtue of a through hole in the cylindrical extension below the flange seat on the mount drilled at 45° relative

Fig. 6. First iteration of new prototype wheel and MTS load test setup. (a) The first new prototype wheel. (b) MTS test frame set up. [Colour online.]



to the wheel rotation axis and held in place by 0.25 in. shoulder bolts that run the entire 2.75 in. width of the hub and fasten into 10-24 stainless steel helical inserts with 0.285 in. installed length. The shoulder bolt heads were countersunk into one of the hub circular faces and the helical inserts installed on the opposite face.

The material selection for the mounts required some carefully managed compromises as the axle bearings in the mounts experience significant cyclical loading during sphere angular manipulation under normal operating conditions. The material needed to have a large strength-to-weight ratio, so 7075 aluminum, a variety of carbon steels, and Grade 5 titanium were selected for trade-off studies. The Grade 5 titanium was the clear choice for its resistance to fatigue and low density of 4.42 g/cm^3 , but the cost for a 1 ft length of 1 in. circular rod stock was US\$162.71. However, the cost for the same-sized 12L14 carbon steel rod, deemed to be the appropriate carbon steel for this application, was an order of magnitude less at US\$20.13. The decision was made to use the titanium for its superior properties despite its high cost per linear foot as only 25.6 linear feet are needed for all 24 passive mecaenum wheels. When given a volume discount, the stock could be obtained for about US\$3800.00, which was deemed affordable. However, as we needed to be absolutely certain of the new design before making the financial investment, we decided to manufacture a single new split-axle passive wheel. To make one wheel, 12.8 in. of titanium rod stock was needed with a cost just a bit more than US\$162.00, so it was decided to order 14 in. to have enough material to absorb what the inevitable lessons machining the titanium would cost. The last feature to consider for the mounts was the rounds at the top of the rectangular tab on the mount containing the hole for the axle bearing. The decision was made to use 0.25 in.

radius rounds for the first prototype and modify, if needed, after load testing the wheels. The passive mecaenum wheel bearings for the 0.5 in. wheel axles were selected to be light-duty ball bearings with a maximum angular speed of 2500 rpm. They can support a maximum of 940 lb_f in dynamic radial load and 850 lb_f in static radial load.

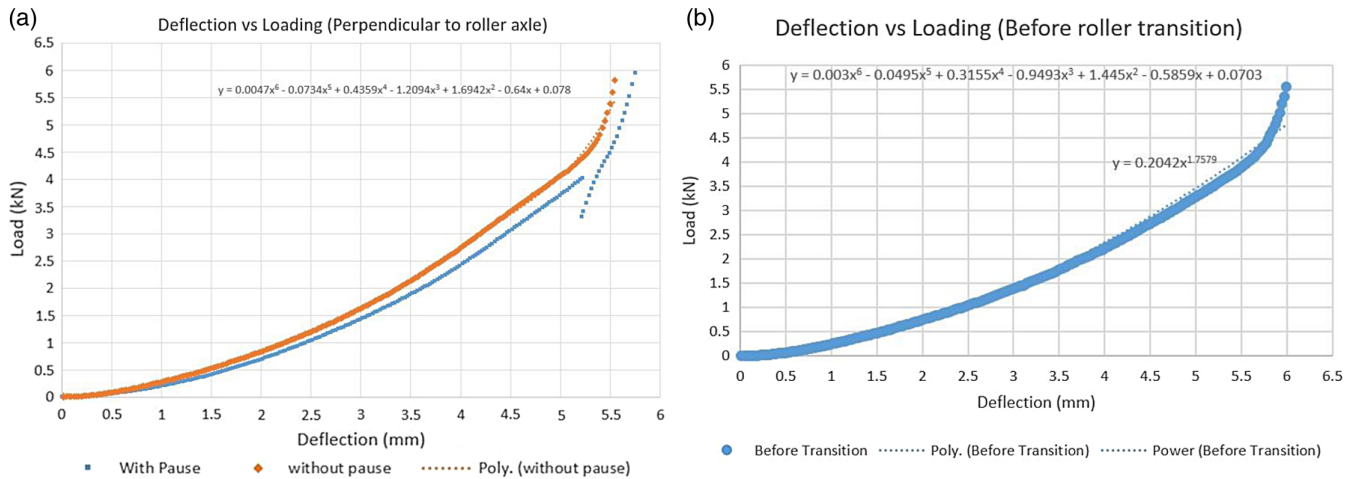
Selection of the castor roller axles converged to 0.25 in. diameter 12L14 carbon steel. Instead of rod stock, 4.00 in. rotary shafts cut to length with adequate diametral dimension tolerance, as well as cylindricity geometric feature tolerances, were selected. The nominal shaft lengths were 3.27 in. for the first prototype. The bearings selected for the roller axles were high-load oil-embedded iron-copper bearings impregnated with SAE 90 oil. The increased iron content makes these bearings stronger and more resistant to shock loads than standard oil-embedded bearings, and they are intended to operate at lower speeds in the range of the estimated maximum passive castor roller angular speeds of 630 rpm, given that the 9.5 ft diameter sphere has a maximum angular speed of approximately 5.83 rpm ($35^\circ/\text{s}$).

The last parts to be considered were the passive rollers. The split-axle design requires two halves of a polyurethane roller with Delrin sleeve bearing surface for the castor roller axle. The decision was made to cut the existing rollers in half. The cutting was done by making a jig to hold a single roller and using a rigidly mounted razor knife blade mounted to an arbour press to shear the rollers. All of the components required were manufactured, and the resulting new prototype was easily assembled and can be seen in Fig. 6a.

2.5. Mecaenum wheel load case analysis

The prototype wheel was tested under load cases it is expected to experience during operation; both quasi-static and dynamic cases were analysed and tested.

Fig. 7. Deflection versus loading curves for different static loading conditions. (a) Static test on one roller, load perpendicular to roller axis. (b) Static test at the transition between two rollers. [Colour online.]



The quasi-static load case determined the maximum loads the wheel could withstand to the point of permanent plastic yielding of relevant components. The dynamic load case provided an estimation of the wheel performance under predicted maximum motion-induced impulsive loads. All tests were completed using an MTS test frame, and the dynamic test set up is illustrated in Fig. 6b, with the base with the same curvature as the sphere outlined. The same set up was used for quasi-static testing, but without a motor connected to the wheel.

2.5.1. Quasi-static load case

The loading was applied gradually by the MTS over a set period of time to collect the data for the deflection of the wheel rollers with respect to the applied load by the MTS. The mecano wheel was loaded and tested in three different orientations, including directly onto one roller perpendicular to the axle, before the transition onto the next roller, and lastly with two rollers evenly sharing the load. The worst loading case was determined to be at the point before transitioning from one roller to the next while the load is at the distal end of one of the rollers. Originally, it was assumed to be the third case, with two rollers evenly sharing the load, but owing to the curvature of the sphere, each mecano wheel roller transitions to the next before reaching the end of the roller.

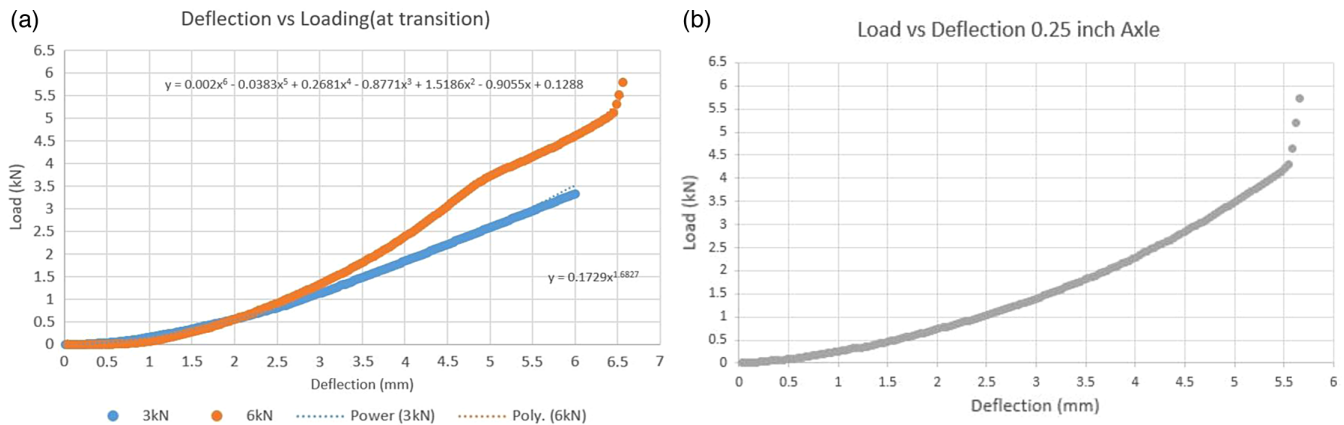
In the estimation of the quasi-static loads the passive wheels experience, momentum changes of the rollers were found to be orders of magnitude smaller than the static loads and were therefore not used in the calculations. The composite sphere has a mass of 907 kg (2000 lb), and the upper halo ring with 12 passive mecano wheel has a mass of 204 kg (450 lb). Three halo ring pneumatic actuators provide 1500 lb downward force to maintain contact between the sphere and the active mecano wheels. Accounting for acceleration of the

sphere, accompanied by the reaction forces of the halo ring and lower active wheels on the sphere, the downward force on the passive mecano wheels was determined to be approximately three times the combined weight of the sphere and halo for a total of 32.7 kN (7350 lb). There are a total of six mounts on the base of the Atlas platform, each with two mecano wheels in rocker panels angled at 45° to the base platform. Accounting for the angle of the mecano wheels and dividing the load among the two wheels per mount, the maximum vertical force on a wheel is 3.9 kN (875 lb). The horizontal load was determined to be 4.4 kN (1000 lb), based on the combination of inertia forces in the vertical and horizontal directions combined with the orientation of the passive wheel mounts and hangars. Considering both the maximum horizontal and vertical loads occurring simultaneously, the mecano wheel design load was established to be 6 kN (1350 lb), yielding a safety factor of 1.3.

The deformation versus load curve was plotted using data points from the MTS, and the trends were similar throughout various setups, see the graphs in Fig. 7. It can be observed that initially the deflection versus loading curve follows a polynomial fit. Once loading approaches approximately 4 kN, the curve begins to increase exponentially. This is very likely attributed to the strain hardening of polyurethane, as more load is applied to the wheel, the polyurethane rollers stiffen (Yakovlev 2016). Figure 7a represents the loading directly onto one roller and shows two different loading conditions for the wheel, one with a pause during loading and one without, to see if a constant load would affect the deflection of the roller.

Figure 7b represents the worst loading case of the wheel, and Fig. 8a represent the loading case when the load is evenly distributed among two rollers loaded up to 3 kN (675 lb) and 6 kN (1350 lb).

Fig. 8. Deflection versus loading curves. (a) Static test with two rollers evenly sharing the load. (b) Titanium axle load versus deflection. [Colour online.]



When loaded to 6 kN (1350 lb), the steel axles failed as a result of permanent plastic deformation. The point at which the axles yielded cannot be differentiated in the deflection versus load graph because of the exponential hardening of the polyurethane rollers. Titanium was the next material to be considered in the design owing to its high strength-to-weight properties with a yield strength of 950 MPa (138 ksi) (Boyer et al. 1994), in both 0.375 and 0.25 in. diameters.

The titanium (Ti-6Al-4V) axles were statically tested and loaded up to 6 kN (1350 lb). Both size axles withstood the loading, and as a result, the 0.25 in. axles were selected. Benefits of the smaller diameter axles are that they are less expensive, lightweight, and have more clearance from the sphere to the end of the axle when loaded. The titanium axle load versus deflection curve followed the same trends as for the steel axles, see Fig. 8b.

2.5.2. Dynamic load cases

When the Atlas motion platform is rotating, the passive mecamum wheels will generally react with their own rotations, both supporting the loads and enabling the motion of the sphere. As a result of this, the passive wheel was tested dynamically to more accurately represent what will happen when in motion. A jig was designed to connect a motor shaft to the wheel allowing it to spin while under load in the MTS, illustrated in Fig. 6b. To conduct this test, a thin strip of plastic was used to slide between the surface of the curved base and the passive rollers. The plastic strip was pulled through during the test to simulate both surfaces moving relative to each other, a stationary surface would cause the rollers to slip on the surface rather than cause castor roller rotation.

While the wheel was spinning, a load was gradually applied to the wheel. At a load of 150 N, the retaining rings deformed and the rollers of the wheel slid off the axle. The proposed redesign of the axles included a threaded step on either end, securing the rollers on the axle with a nut. The new design was tested, and the

wheel was loaded to the maximum force the driving motor could support of 0.5 kN (112 lb). The wheel was running at 75 rpm, which is equivalent to the sphere spinning at 3 rpm, and it did not fail.

Both the static and dynamic tests provided important data to finalise the split-axle mecamum wheel design. There were design changes that resulted from both sets of test data analysis that will be further discussed in the following section. Note that creep tests were not conducted, as tests satisfied the maximum loading for any appreciable amount of time, and creep was therefore not considered in this paper.

2.6. Final passive mecamum wheel prototype

The first split-axle prototype wheel had an overall diameter of 13.3 cm (5.25 in.) because of tolerance stack-ups and had to be reduced to 12.7 cm (5 in.) to fit in the existing mounts for the wheels. To account for the 0.64 cm (0.25 in.), the countersink for the mount on the hub was increased and the shoulder height of the mount was decreased. The corners of the titanium mounts were rounded to an increased radius of 0.375 in., allowing for an increased clearance when the roller is compressed to the sphere. Additionally, recommendations from the initial assembly process were taken into consideration for the new design tolerances.

An initial static test was conducted with the prototype's steel axles, which permanently deformed when loaded to 4 kN (900 lb); however, they needed to withstand 6 kN (1350 lb), resulting in a material change from steel to titanium. The dynamic test of the mecamum wheel showed that c-clip retaining rings on the ends of the axles were not sufficient to keep the rollers on the axles. The c-clip retaining rings deformed from the force of the polyurethane pressing against them, and the rollers slipped out of the axles under minimal loading. The axles were redesigned with a step on either end to secure the rollers on the axle with nuts. The new axle design was tested dynamically and did not fail

Fig. 9. Final split-axle passive mecanum wheel. [Colour online.]



under the maximum load of 0.5 kN (112 lb) that could be applied by the motor used for the test that was spinning the wheel. Figure 9 shows the final passive mecanum wheel prototype design.

3. Conclusions

In this paper, we have outlined the design path that has led to the first truly acceptable split-axle passive mecanum wheel prototype, which will be manufactured and used to both provide adequate tractive force between the sphere and active mecanum wheels for rotational actuation as well as to help distribute the resulting static and dynamic loads. Several critical functional operation deficiencies in the original twin-hub prototypes were identified. A variety of alternate solutions were investigated, leading to the realisation that a split-axle design was likely the best design option to resolve the functional deficiencies. The first split-axle design was iteratively developed, and a new prototype was manufactured. Empirical tests identified load capacity deficiencies in the passive roller axle materials and design. Decisions were made to correct the deficiencies, and an updated split-axle passive wheel prototype was designed and manufactured. Results of further load tests indicated that the second split-axle prototype either met or exceeded all operational and functional requirements.

Acknowledgements

The authors are grateful for contributions to this work by the staff of the Machine Shop in the Department of Mechanical and Aerospace Engineering at Carleton University, in particular Machinist Kevin Sangster, as

well as Supervisor Alex Proctor. Additionally, Laboratory Technologist Steve Truttmann was heavily involved with the design and implementation of multiple pieces of test apparatus and data gathering. Finally, Professor Marc Arsenault of Laurentian University generously provided the French translation.

References

- Bles, W., Hosman, R.J.A.W., and de Graff, B. 2000. Desdemona - advanced disorientation trainer and (sustained-g) flight simulator. AIAA Modeling and Simulation Technologies Conference, Denver, CO, USA.
- Boyer, R., Welsch, G., and Collings, E.W. 1994. Materials properties handbook: titanium alloys. ASM International, Materials Park, OH, USA.
- Chao, H.C., Pearce, T.W., and Hayes, M.J.D. 2004. Use of the HLA in a real-time multi-vehicle simulator. Proc. CSME Forum 2004, University of Western Ontario, London, ON, Canada, 1–4 June 2004.
- Gfrerrer, A. 2008. Geometry and kinematics of the Mecanum wheel. *Comput. Aided Geom. Des.* **25**(9): 784–791. doi:[10.1016/j.cagd.2008.07.008](https://doi.org/10.1016/j.cagd.2008.07.008).
- Gough, V.E. 1956. Discussion in London: automobile stability, control, and tyre performance. Proc. Automobile Division, Institution of Mech. Engrs., pp. 392–394.
- Hayes, M.J.D., and Langlois, R.G. 2005. Atlas: a novel kinematic architecture for six DOF motion platforms. *Trans. Can. Soc. Mech. Eng.* **29**: 701–709. doi:[10.1139/tcsme-2005-0047](https://doi.org/10.1139/tcsme-2005-0047).
- Holland, J.B., Hayes, M.J.D., and Langlois, R.G. 2005. A slip model for the spherical actuation of the atlas motion platform. *Trans. Can. Soc. Mech. Eng.* **29**: 711–720. doi:[10.1139/tcsme-2005-0048](https://doi.org/10.1139/tcsme-2005-0048).
- IEEE Standard. 2000. Standard for modeling and simulation for high level architecture (HLA). IEEE 1516-2000.
- Ilon, B.E. 1975. Control of an omni-directional robotic vehicle with mecanum wheels. US Patent 3876255.
- Kim, J., Hwang, J.C., Jim, J.S., Iurascu, C.C., Park, F.C., and Cho, Y.M. 2002. Eclipse II: a new parallel mechanism enabling continuous 360-degree spinning plus three-axis translational motions. *IEEE Transactions on Robotics and Automation*, **18**(3): 367–373. doi:[10.1109/TRA.2002.1019472](https://doi.org/10.1109/TRA.2002.1019472).
- Plumpton, J.J., Hayes, M.J.D., Langlois, R.G., and Burlton, B.V. 2014. Atlas motion platform mecanum wheel Jacobian in the velocity and static force domains. *Trans. Can. Soc. Mech. Eng.* **38**: 251–261. doi:[10.1139/tcsme-2014-0018](https://doi.org/10.1139/tcsme-2014-0018).
- Pond, G., and Carretero, J.A. 2007. Quantitative dexterous workspace comparison of parallel manipulators. *Mech. Mach. Theory*, **42**(10): 1388–1400. doi:[10.1016/j.mechmachtheory.2006.10.004](https://doi.org/10.1016/j.mechmachtheory.2006.10.004).
- Robinson, J.D., Holland, J.B., Hayes, M.J.D., and Langlois, R.G. 2005. Velocity-level kinematics of the atlas spherical orienting device using omni-wheels. *Trans. Can. Soc. Mech. Eng.* **29**: 691–700. doi:[10.1139/tcsme-2005-0046](https://doi.org/10.1139/tcsme-2005-0046).
- Stewart, D. 1965. A platform with six degrees of freedom. *Proc. Inst. Mech. Eng.* **180**(15): 371–386. doi:[10.1243/PIME_PROC_1965_180_029_02](https://doi.org/10.1243/PIME_PROC_1965_180_029_02).
- Wallenberger, F.T., and Bingham, P.A., (eds.). 2010. Fiberglass and glass technology: energy-friendly compositions and applications. Springer-Verlag, New York, NY, USA.
- Yakovlev, S.N. 2016. Dynamic hardening of structural polyurethanes. *Russ. Eng. Res.* **36**(4): 255–257. doi:[10.3103/S1068798X16040213](https://doi.org/10.3103/S1068798X16040213).